The influence of pore size on osteoblast phenotype expression in cultures grown on porous titanium

Teixeira, L. N.; Crippa, G. E.; Lefebvre, L.-P.; De Oliveira, P. T.; Rosa, A. L.; Beloti, M. M.

Publisher's version / Version de l'éditeur:
https://doi.org/10.1016/j.ijom.2012.02.020
International Journal of Oral and Maxillofacial Surgery, 41, 9, pp. 1097-1101, 2012-04-08

The influence of pore size on osteoblast phenotype expression in cultures grown on porous titanium

ABSTRACT

Objective: This study aimed at investigating the effect of pore size on osteoblastic phenotype development in cultures grown on porous titanium (Ti). Material and methods: Porous Ti discs with three different pore sizes, 312 μm (Ti 312), 130 μm (Ti 130) and 62 μm (Ti 62) were fabricated by powder metallurgy process. Osteoblastic cells obtained from human alveolar bone were cultured on porous Ti samples for periods of up to 14 days. Results: Cell proliferation was affected by pore size at day 3 ($p=0.0010$), day 7 ($p=0.0005$) and day 10 ($p=0.0090$) at the following way: Ti 62 < Ti 130 < Ti 312. Gene expression of bone markers evaluated at 14 days was affected, *RUNX2* ($p=0.0153$), *ALP* ($p=0.0153$), *BSP* ($p=0.0156$), *COL* ($p=0.0156$), and *OPN* ($p=0.0156$) by pore size as following: Ti 312 < Ti 130 < Ti 62. Conclusion: Based on these results, we may suggest that porous Ti surfaces with pore size nearby 62 μm, compared with 312 μm and 130 μm, yield the higher expression of osteoblast phenotype as indicated by lower cell proliferation rate as well as higher gene expression of bone markers.

Key words: Cell culture. Osteoblast. Implant. Pore size. Porous titanium.

INTRODUCTION

Over the past 40 years, Ti has been considered the gold standard biomaterial to fabricate implants for dental and orthopedic purposes. Classically, implant fixtures are prepared with bulk Ti varying surface morphology and despite the high rate of success, limitations like interfacial instability with host tissues, and lack of biological anchorage have been reported[1-3]. Thus, approaches to improve bone-implant fixation, mainly in critical bone sites, remain an absorbing topic in implantology with porous biomaterials rising to provide anchorage by favoring ingrowth of mineralized tissue into the pores[4-6].

The powder metallurgy process is able to produce Ti foams with adjustment of the pore size within the range required for bone ingrowth[7,8]. In previous study, we have shown the development of osteoblast phenotype of cells cultured on porous Ti produced by this method[9]. Also, our data revealed that the thickness of the porous Ti coating affects the osteoblast phenotype expression[10]. Several works have suggested that porous biomaterials should present adequate interconnected pore size to allow the formation of a new vascular system for continuing bone ingrowth[1,11-13]. Implants with a pore size range from 50 to 400 μm have been considered acceptable to allow biological anchorage[14]. However, up to now, there is no consensus on the optimal pore size to yield the ideal tissue response. Based on this, the present study was designed to evaluate the osteoblast phenotype expression of human alveolar bone-derived cells grown on porous Ti with three different pore sizes.

MATERIAL AND METHODS

Porous Ti preparation

Porous Ti foams were produced as described elsewhere[8]. Ti powder was dry-mixed with a polyethylene binder and a chemical foaming agent (p,p'-oxybis[benzenesulfonyl hydrazide]). This mixture was poured into a mold and foamed at 210°C in air. The resulting material was then debinded at 450°C in air and presintered under vacuum at 1000°C, with three different pore sizes, 312 μm (Ti 312) 130 μm (Ti 130), and 62 μm (Ti 62), and the same porosity of 60%. All samples were then machined to obtain discs with 12 mm diameter. The discs were washed for 15 min in acetone in an ultrasonic bath (Bandelin Sonorex, Amtrex Technologies Inc., St. Laurent, Quebec, Canada). Finally, the porous specimens were sintered at 1400°C to consolidate the material and autoclaved at 120°C for 40 min before using in the cell culture experiments.

Cell culture

Human alveolar bone fragments (explants) from two healthy donors were used under the rules of the Committee of Ethics in Research of the School of Dentistry of Ribeirao Preto – University of Sao Paulo. Osteogenic cells were harvested from these explants by enzymatic digestion using type II collagenase (Gibco – Life Technologies, Grand Island, NY, USA) as described elsewhere[15,16]. These cells were cultured in α-minimum essential medium (Gibco), supplemented with 10% foetal bovine serum (Gibco), 50 µg/mL gentamicin (Gibco), 0.3 µg/mL fungisone (Gibco), 10^{-7} M dexamethasone (Sigma, St. Louis, MO, USA), 5 µg/mL ascorbic acid (Gibco), and 7 mM β-glycerophosphate (Sigma) until subconfluence. First passaged cells were cultured in 24-well culture plates (Falcon, Franklin Lakes, NJ, USA) on porous Ti samples at a cell density of 2×10^4 cells/sample. Cultures were kept at 37°C in a humidified atmosphere of 5% CO_2 and 95% air; the medium was changed every 3 or 4 days.

Fluorescence labelling

At day 3, cells were fixed for 10 min at room temperature using 4% paraformaldehyde in 0.1 M phosphate buffer (PB), pH 7.2. Cells were permeabilised with 0.5% Triton X-100 in PB for 10 min followed by blocking with 5% skimmed milk in PB for 30 min. Primary antibody to human Ki-67 (polyclonal, 1:70; Diagnostic Biosystems, Pleasanton, CA, USA) was used, followed by Alexa Fluor 594 (red fluorescence)-conjugated goat anti-rabbit secondary antibody (1:200; Molecular Probes, Invitrogen, Eugene, OR, USA). Alexa Fluor 488 (green fluorescence)-conjugated phalloidin (1:200, Molecular Probes) was used to label actin cytoskeleton. All antibody incubations were performed in a humidified environment for 60 min at room temperature. Cell nuclei were stained with 300 nM 4',6-diamidino-2-phenylindole, dihydrochloride (DAPI, Molecular Probes) for 5 min. Porous Ti samples were mounted face up on glass slides and a glass coverslip was mounted with an antifade kit (Vectashield, Vector Laboratories, Burlingame, CA, USA) on the surface containing cells. The samples were then examined by using a fluorescence microscope (Leica, Bensheim, Germany) outfitted with a Leica DC 300F digital camera under epifluorescence. The acquired digital images were processed with Adobe Photoshop software.

Culture growth

Culture growth was evaluated at days 3, 7, and 10 by 3-[4,5-dimethylthiazol-2-yl]-

2,5- diphenyl tetrazolium bromide (MTT) assay. Cells were incubated with 100 μL of MTT (5 mg/mL) in PBS at 37°C for 4 and after that, 1 mL of acid isopropanol (0.04 N HCl in isopropanol) was added to each well. The plates were then stirred for 5 min, and 100 μL of this solution were used to read the optical density at 570 nm on the plate reader (μQuant, Biotek, Winooski, VT, USA) and data were expressed as absorbance. To avoid any background, samples of porous Ti were kept in culture medium without cells and assayed to subtract the absorbance from experiments carried out with cells.

Real-time reverse transcriptase-polymerase chain reaction (real-time PCR)

At 14 days, gene expression of runt-related transcription factor 2 (*RUNX2*), alkaline phosphatase (*ALP*), bone sialoprotein (*BSP*), type I collagen (*COL*), and osteopontin (*OPN*) were evaluated by real-time PCR. Primers were designed with Primer Express 2.0 (Applied Biosystems, Foster City, CA, USA) and are shown in Table 1.

Total RNA was extracted using the Promega RNA extraction kit (Promega, Madison, WI, USA), according to the manufacturer instructions. Complementary DNA (cDNA) was synthesized using 2 µg of RNA through a reverse transcription reaction (M–MLV reverse transcriptase, Promega). Real-time PCR was carried out in an ABI Prism 7000 Sequence Detection System using the SybrGreen system (Applied Biosystems, Warrington, UK). SybrGreen PCR MasterMix (Applied Biosystems), specific primers and 2.5 ng cDNA were used in each reaction. The standard PCR conditions were 95°C (10 min) and 40 cycles of 94°C (1 min), 56°C (1 min) and 72°C (2 min), followed by the standard denaturation curve. To mRNA analysis, the relative level of gene expression was calculated in reference to β–actin expression and normalized by the gene expression of cells cultured on polystyrene using the cycle threshold (Ct) method.

Statistical analysis

Quantitative data for cell culture experiments presented in this work are the representative results of two separate experiments using two sets of cultures established from two different donors. Experiments of culture growth were carried out in quintuplicate (n=5) and gene expression, in triplicate (n=3). Analyses were done using Kruskal-Wallis test followed by Fischer test based on rank, comparing all surfaces for each time point (level of significance: 5%).

RESULTS

Adherent cells were spread and distributed throughout the surfaces of all porous Ti as evidenced by actin cytoskeleton labelling at day 3 (Figure 1A–C). No relevant differences among the three pore sizes were noticed and the majority of cells on Ti samples presented a spread polygonal shape. Clearly, the spherical features of porous surfaces affected cell morphology, as some cells edged the perimeter of the spheres. Immunolabelled preparations with an anti-Ki67 antibody revealed that at day 3 all surfaces presented a high proportion of cells in proliferative activity.

Culture growth analyses indicated that cell number increased from day 3 to 10, irrespective to the pore size and cell proliferation was affected by surfaces in all time points (day 3 – $p=0.0010$; day 7 – $p=0.0005$; day 10 – $p=0.0090$) at the following way: Ti 62 < Ti 130 < Ti 312 (Figure 2).

Gene expression of all osteoblast markers evaluated at 14 days was affected, *RUNX2* ($p=0.0153$), *ALP* ($p=0.0153$), *BSP* ($p=0.0156$), *COL* ($p=0.0156$), and *OPN* ($p=0.0156$) by pore size as following: Ti 312 < Ti 130 < Ti 62 (Figure 3).

DISCUSSION

Previously, we have shown that porosity is a determinant feature of Ti surface to modulate osteoblast differentiation[9,10]. Here, aiming to extend this investigation, we have evaluated the influence of pore size on osteoblast phenotype expression in cultures grown on porous Ti with three different pore size averages 62 µm (Ti 62), 130 µm (Ti 130), and 312 µm (Ti 312). The outcomes indicated that surfaces with 62-µm-pore size yield the higher expression of osteoblast phenotype.

The progression of tissue-implant interactions is primarily in need of cell migration and adhesion on substrate and because of that such events are focused in a wide range of studies in the field of biomaterials[17,18]. In the present study, porous Ti surfaces with different pore sizes supported similar patterns of cell spreading, as observed by epifluorescence of actin cytoskeleton labelling. Indeed, the architecture of porous Ti, exhibiting interconnected spheres, drove cell morphology and undoubtedly affected the in vitro tissue ingrowth as previously noticed[9].

Following adhesion, cells entry into the proliferative phase to colonize the implant surface and it has been reported that porous biomaterials represent an advantageous milieu for cell growth. Cultures of human alveolar bone-derived cells presented a higher proliferation rate on totally porous or porous coating Ti compared to dense one[10-11]. The same findings have been noticed for both newborn mouse calvaria-

derived MC3T3-E1 pre-osteoblastic cells and human osteosarcoma cell lineage MG63[7,19]. In line with these observations, here, we observed a high proportion of cells in proliferative activity on the three porous Ti surfaces by using anti-Ki67 antibody. In addition, cell proliferation evaluated by the reduction of MTT by the mitochondrial dehydrogenase of viable cells was progressively higher on surfaces with bigger pore size. This increase of cell proliferation could be attributed to the three-dimensional design of porous structures, which mimic the trabecular bone, favoring tissue ingrowth, and to the more surface area available for cell growth[2,9,20].

The gene expression of *RUNX2*, *ALP*, *BSP*, *COL*, and *OPN*, key markers of bone tissue, was used to evaluate the development of osteoblast phenotype. As extensively reported, RUNX2 is the master transcriptional factor that initiate bone formation[21]. The enzyme ALP hydrolyzes pyrophosphates, releasing inorganic phosphate to promote mineralization of the extracellular matrix, which is composed primarily of COL[22,23]. BSP and OPN are non-collagenous matrix proteins involved in nucleation of hydroxyapatite crystals, and inhibition of mineralization and regulation of cell-matrix and matrix-matrix adhesion, respectively[24,25]. It is worthy of note that, for all evaluated genes the smaller was the pore size the higher was the gene expression, contrasting the cell proliferation profile, where bigger pore size up-regulated culture growth. These findings of osteoblast gene expression and cell proliferation are supported by the reciprocal relationship between the decrease in culture growth and the induction of cell differentiation reported elsewhere[26,27].

CONCLUSION

Our results suggest that porous Ti surfaces with pore size average around 62 μm elicit the higher expression of osteoblast phenotype as indicated by lower cell proliferation rate as well as higher gene expression of bone markers. In addition to pore size, the thickness of the porous Ti coating may affect osteoblast differentiation[10]. Taken together, these observations could contribute to the development of Ti implant surfaces with the ideal pore size and thickness to yield osseointegration in challenging bone sites.

ACKNOWLEDGEMENTS

This work was supported by the National Council of Scientific and Technological Development (CNPq, Brazil) and Sao Paulo Research Foundation (FAPESP, Brazil).

We would like to thank Fabíola S. de Oliveira, Roger R. Fernandes, and Junia Ramos for the helpful assistance they provided during the cell culture experiments.

REFERENCES

1. Li JP, Habibovic P, van den Doel M, Wilson CE, de Wijn JR, van Blitterswijk CA, et al. Bone ingrowth in porous titanium implants produced by 3D fiber deposition. Biomaterials. 2007;28:2810-20.
2. Pilliar RM. Powder metal-made orthopedic implants with porous surface for fixation by tissue ingrowth. Clin Orthop Relat Res. 1983;176:42-51.
3. Pilliar RM, Cameron HU, Welsh RP, Binnington AG. Radiographic and morphologic studies of load-bearing porous-surfaced structured implants. Clin Orthop and Relat Res. 1981;156: 249-57.
4. Maniatopoulos C, Pilliar RM, Smith DC. Threaded versus porous surfaced designs for implant stabilization in bone-endodontic implant model. J Biomed Mater Res. 1986,20:1309-33.
5. Murray GA, Semple JC. Transfer of tensile loads from a prosthesis to bone using porous titanium. J Bone Joint Surg Br. 1981;63-B:138-41.
6. Pilliar RM, Cameron HU, Macnab I. Porous surface layered prosthetic devices. Biomed Eng. 1975;10:126-31.
7. St-Pierre JP, Gauthier M, Lefebvre LP, Tabrizian M. Three-dimensional growth of differentiating MC3T3-E1 pre-osteoblasts on porous titanium scaffolds. Biomaterials. 2005;26:7319-28.
8. Lefebvre LP, Thomas Y. Method of making open cell material. US Patent No. 6660224, 2003.
9. Rosa AL, Crippa GE, de Oliveira PT, Taba Jr M, Lefebvre LP, Beloti MM. Human alveolar bone cell proliferation, expression of osteoblastic phenotype, and matrix mineralization on porous titanium produced by powder metallurgy. Clin Oral Implants Res. 2009;20:472-81.
10. Canabarro A, Crippa GE, Shirozaki MU, Sampaio EM, Lefebvre LP, de Oliveira PT, et al. Effect of porous titanium coating thickness on in vitro osteoblast phenotype expression. J Osseoint. 2011;1:35-41.
11. Sicchieri LG, Crippa GE, de Oliveira PT, Beloti MM, Rosa AL. Pore size regulates cell and tissue interactions with PLGA-CaP scaffolds used for bone engineering. J Tissue Eng Regen Med. 2011;doi: 10.1002/term.422.
12. Pamula E, Bacakova L, Filova E, Buczynska J, Dobrzynski P, Noskova L, et al.

The influence of pore size on colonization of poly(L-lactide-glycolide) scaffolds with human osteoblast-like MG 63 cells in vitro. J Mater Sci Mater Med. 2008; 19:425-35.

13. Li JP, de Wijn JR, van Blitterswijk CA, de Groot K. Porous Ti6Al4V scaffolds directly fabricated by 3D fibre deposition technique: effect of nozzle diameter. J Mater Sci Mater Med. 2005;16:1159-63.
14. Bobyn JD, Pilliar RM, Cameron HU, Weatherly GC. The optimum pore size for the fixation of porous-surfaced metal implants by the ingrowth of bone. Clin Orthop. 1980;150:263-70.
15. Beloti MM, de Oliveira PT, Gimenes R, Zaghete MA, Bertolini MJ, Rosa AL. In vitro biocompatibility of a novel membrane of the composite poly(vinylidene-trifluoroethylene)/barium titanate. J Biomed Mater Res A. 2006;79:282-8.
16. Beloti MM, Martins Jr W, Xavier SP, Rosa AL. In vitro osteogenesis induced by cells derived from sites submitted to sinus grafting with anorganic bovine bone. Clin Oral Implants Res. 2008;19:48-54.
17. Saldaña L, Vilaboa N. Effects of micrometric titanium particles on osteoblast attachment and cytoskeleton architecture. Acta Biomater. 2010;6:1649-60.
18. Passeri G, Cacchioli A, Ravanetti F, Galli C, Elezi E, Macaluso GM. Adhesion pattern and growth of primary human osteoblastic cells on five commercially available titanium surfaces. Clin Oral Implants Res. 2010;21:756-65.
19. Simon M, Lagneau C, Moreno J, Lissac M, Dalard F, Grosgogeat B. Corrosion resistance and biocompatibility of a new porous surface for titanium implants. Eur J Oral Sci. 2005;113:537-45.
20. Holy CE, Fialkov JA, Davies JE, Shoichet MS. Use of a biomimetic strategy to engineer bone. J Biomed Mat Res A. 2003;15:447-53.
21. Lian JB, Stein GS, Javed A, van Wijnen AJ, Stein JL, Montecino M, et al. Networks and hubs for the transcriptional control of osteoblastogenesis. Rev Endocr Metab Disord. 2006;7:1-16.
22. Whyte MP. Hypophosphatasia and the role of alkaline phosphatase in skeletal mineralization. Endocr Rev. 1994;15:439-61.
23. Whyte MP. Physiological role of alkaline phosphatase explored in hypophosphatasia. Ann N Y Acad Sci. 2010;1192:190-200.
24. Ganss B, Kim RH, Sodek J. Bone sialoprotein. Crit Rev Oral Biol Med. 1999;10:79-98.
25. McKee MD, Nanci A. Osteopontin at mineralized tissue interfaces in bone,

teeth, and osseointegrated implants: ultrastructural distribution and implications for mineralized tissue formation, turnover, and repair. Microsc Res Tech. 1996;33:141-64.

26. Owen TA, Aronow M, Shalhoub V, Barone LM, Wilming L, Tassinari MS, et al. Progressive development of the rat osteoblast phenotype in vitro: reciprocal relationships in expression of genes associated with osteoblast proliferation and differentiation during formation of the bone extracellular matrix. J Cell Physiol. 1990;143:420-30.
27. Rosa AL, Beloti MM. TAK-778 enhances osteoblast differentiation of human bone marrow cells via an estrogen-receptor-dependent pathway. J Cell Biochem. 2004;91:749-55.

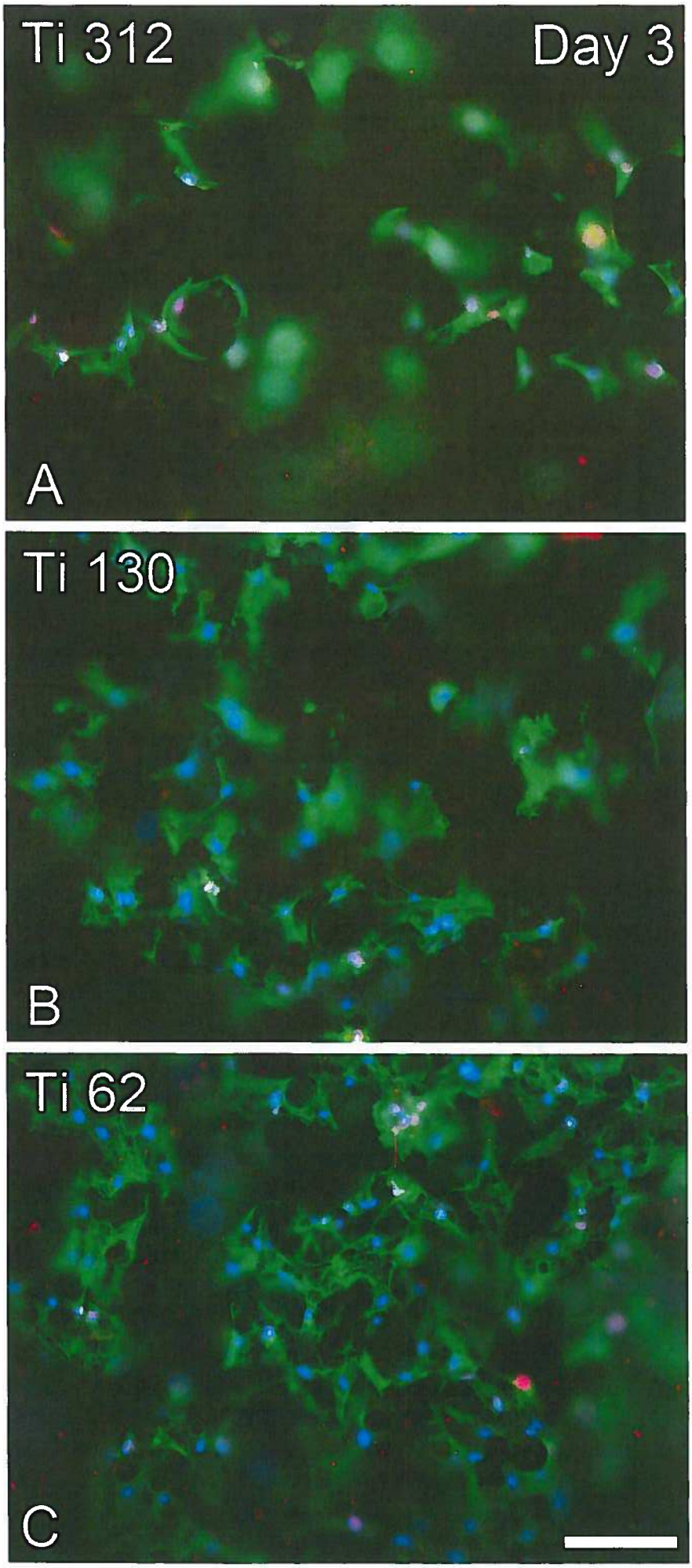
Ti 312
Day 3
A
Ti 130
B
Ti 62
C

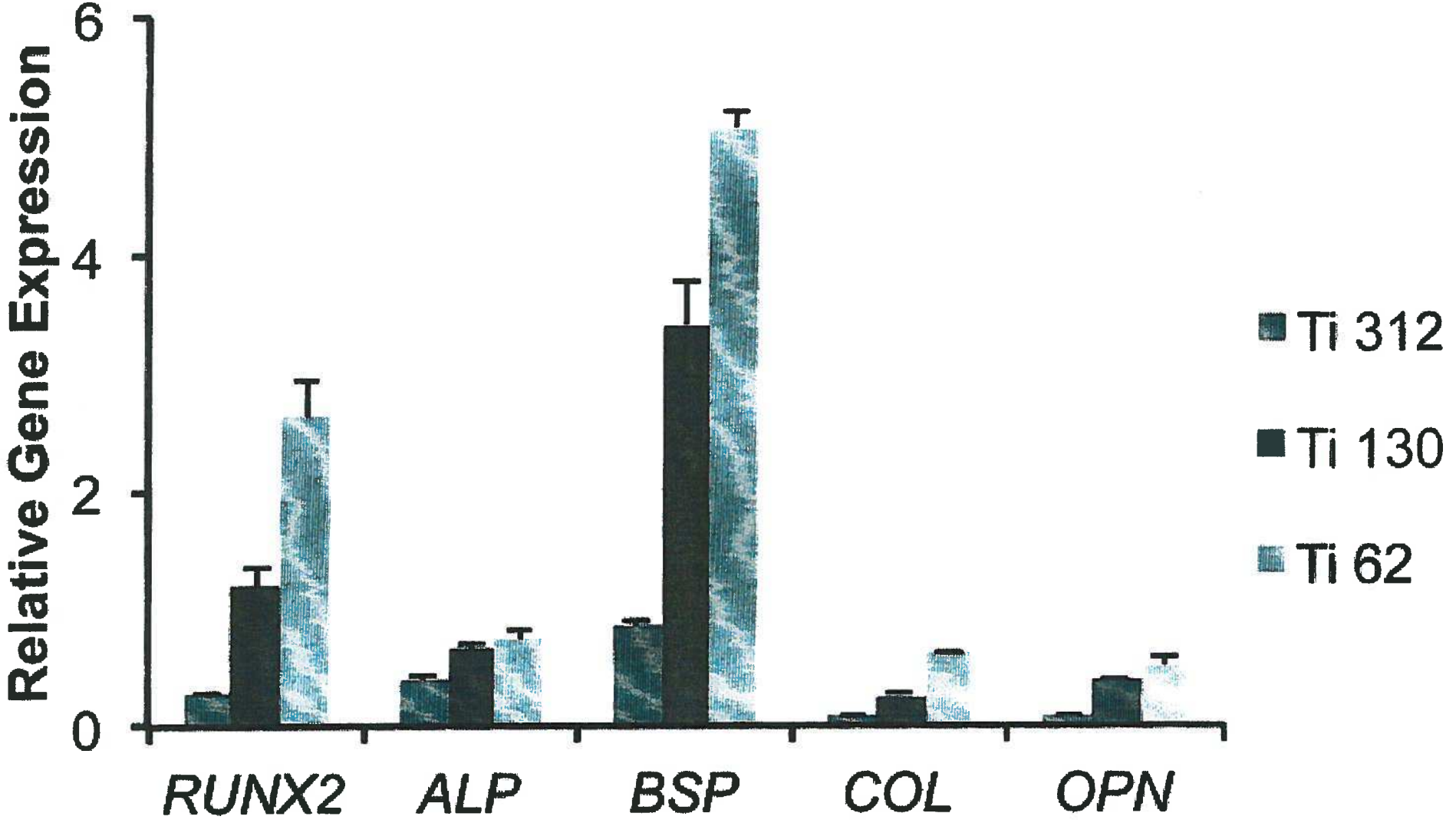
Relative Gene Expression
6
4
2
0
RUNX2
ALP
BSP
COL
OPN
Ti 312
Ti 130
Ti 62

TABLE 1. Primer Sequences, Melting Temperature (TM), and Product Size (bp) for Real-Time PCR Reactions

Gene*	Sequência *primer sense* Sequência *primer anti-sense*	TM (°C)	bp
RUNX2	TATGGCACTTCGTCAGGATCC AATAGCGTGCTGCCATTCG	83	110
ALP	ACGTGGCTAAGAATGTCATC CTGGTAGGCGATGTCCTTA	86	475
BSP	AATCTGTGCCACTCACTGCCTT CCTCTATTTTGACTCTTCGATGCAA	79	201
COL	CCACAAAGAGTCTACATGTCTAGGGTC GTCATCGCACAACACCTTGC	84	114
OPN	AGACACATATGATGGCCGAGG GGCCTTGTATGCACCATTCAA	79	154
β-ACTIN	ATGTTTGAGACCTTCAACA CACGTCAGACTTCATGATGG	75	495

Runt-related transcription factor 2 (*RUNX2*), alkaline phosphatase (*ALP*), bone sialoprotein (*BSP*), collagen type I (*COL*), and osteopontin (*OPN*). For all primers, anneling temperature was 60°C.